

LCCM-VC: LEARNED CONDITIONAL CODING MODES FOR VIDEO CODING*Hadi Hadizadeh and Ivan V. Bajić*

School of Engineering Science, Simon Fraser University, Burnaby, BC, Canada

ABSTRACT

End-to-end learning-based video compression has made steady progress over the last several years. However, unlike learning-based image coding, which has already surpassed its handcrafted counterparts, learning-based video coding still has some ways to go. In this paper we present learned conditional coding modes for video coding (LCCM-VC), a video coding model that achieves state-of-the-art results among learning-based video coding methods. Our model utilizes conditional coding engines from the recent conditional augmented normalizing flows (CANF) pipeline, and introduces additional coding modes to improve compression performance. The compression efficiency is especially good in the high-quality/high-bitrate range, which is important for broadcast and video-on-demand streaming applications. We will provide the code of the proposed model at www.github.com upon completion of the review process.

Index Terms— End-to-end video coding, conditional coding, augmented normalizing flows, autoencoders

1. INTRODUCTION

With the rapid advancement of deep learning technologies, various end-to-end learned image/video codecs have been developed [1, 2, 3] to rival their handcrafted counterparts such as JPEG, High Efficiency Video Coding (HEVC) [4], and Versatile Video Coding (VVC) [5]. For instance, in the seminal work by Ballé *et al.* [1], the variational autoencoders (VAE) were used to construct an end-to-end learned image compression system based on a context-adaptive entropy model. This model incorporates a hyperprior as side information to effectively capture dependencies in the latent representation, thereby improving entropy modeling. Many follow-up VAE-based models were then developed to further improve compression performance [2, 6, 3]. A popular one by Cheng *et al.* [3] used discretized Gaussian mixture likelihoods to parameterize the latent distribution for entropy modeling, achieving high rate-distortion (RD) performance. In fact, the results in [3] show that this model achieves superior performance on both PSNR and MS-SSIM quality metrics

over JPEG, JPEG2000, and HEVC (Intra), and comparable performance with VVC (Intra).

Although VAEs have been proven to be effective for image compression, their ability to provide high-quality input reconstruction has been called into question [7]. To address this issue, a learned lossy image compression method was proposed in [7] based on normalizing flows. Using augmented normalizing flows (ANF), Ho *et al.* [8] developed ANF for image compression (ANFIC), which combines both VAEs and normalizing flows to achieve the state-of-the-art performance for image compression, even better than [3].

Building on the success of learned image compression, learned video compression is catching up quickly. Lu *et al.* [9] presented deep video compression (DVC) as the first end-to-end learned video codec based on temporal predictive coding. Agustsson *et al.* [10] proposed an end-to-end video coding model based on a learning-based motion compensation framework in which a warped frame produced by a learned flow map is used a predictor for coding the current video frame. Liu *et al.* [11] used feature-domain warping in a coarse-to-fine manner for video compression. Hu *et al.* [12] employed deformable convolutions for feature warping.

Most of the existing video codecs rely on residual coding. However, Ladune *et al.* [14, 15] argued that conditional coding relative to a predictor is more efficient than residual coding using the same predictor. Building on this idea, Ho *et al.* [16] proposed conditional augmented normalizing flows for video coding (CANF-VC), which achieves state-of-the-art performance among learned video codecs. CANF-VC uses conditional coding for both motion and inter-frame coding.

In this paper we extend these ideas further. First, we provide a more comprehensive theoretical justification for conditional coding relative to multiple predictors/coding modes. Then, using conditional coding engines from CANF-VC, we construct a codec called learned conditional coding modes for video coding (LCCM-VC). The results show that LCCM-VC outperforms CANF-VC on three commonly used video test sets, and even outperforms HM 16.22 [17] implementation of HEVC on two out of three of these datasets.

The paper is organized as follows. The proposed system is presented in Section 2, including its theoretical motivation in Section 2.1 and implementation description in Section 2.2. Experiments are described and analyzed in Section 3. Finally, the conclusions are drawn in Section 4.

This work was supported in part by the Natural Sciences and Engineering Research Council (NSERC) of Canada and by Compute Canada.

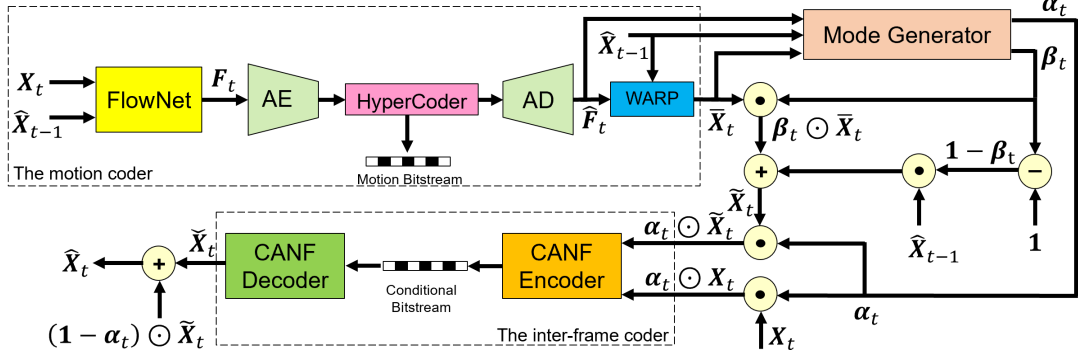


Fig. 1. The block diagram of the proposed learned video compression system. AE and AD are the encoder and decoder of the HyperPrior coder from [1], respectively, and \odot is point-wise multiplication. What is shown is the encoding of the first P frame where we use the HyperPrior coder for motion coding. We use PWC-Net [13] as the FlowNet.

2. PROPOSED METHOD

2.1. Motivation

We motivate the proposed codec via information theory. Let X and Y be two random variables and let $R = X - Y$, then

$$\begin{aligned} H(X|Y) &= H(R + Y|Y) \stackrel{(a)}{=} H(R|Y) \\ &\stackrel{(b)}{\leq} H(R) = H(X - Y), \end{aligned} \quad (1)$$

where $H(\cdot)$ is the entropy, $H(\cdot|\cdot)$ is the conditional entropy, (a) follows from the fact that given Y , the only uncertainty in $R + Y$ is due to R , and (b) follows from the fact that conditioning does not increase entropy [18].

Now consider the following Markov chain $X \rightarrow Y \rightarrow f(Y)$ where $f(\cdot)$ is an arbitrary function. By the data processing inequality [18], we have $I(X; f(Y)) \leq I(X; Y)$, where $I(\cdot; \cdot)$ is the mutual information. Expanding the two mutual informations as follows: $I(X; f(Y)) = H(X) - H(X|f(Y))$ and $I(X; Y) = H(X) - H(X|Y)$, and applying the data processing inequality, we conclude

$$H(X|Y) \leq H(X|f(Y)). \quad (2)$$

In video compression, coding modes are constructed via predictors, for example inter coding modes use other frames to predict the current frame, while intra coding modes use information from the same frame to form a prediction. Let $X = \mathbf{X}_t$ be the current frame, $Y = \{\mathbf{X}^{(1)}, \dots, \mathbf{X}^{(n)}\}$ be a set of n candidate predictors, and $\mathbf{X}_p = f(\mathbf{X}^{(1)}, \dots, \mathbf{X}^{(n)})$ be a predictor for \mathbf{X}_t from $\{\mathbf{X}^{(1)}, \dots, \mathbf{X}^{(n)}\}$. Function $f(\cdot)$ could, for example, use different combinations of $\{\mathbf{X}^{(1)}, \dots, \mathbf{X}^{(n)}\}$ in different regions of the frame. Then, based on (1) and (2),

$$\begin{aligned} H(\mathbf{X}_t|\mathbf{X}^{(1)}, \dots, \mathbf{X}^{(n)}) &\leq H(\mathbf{X}_t|f(\mathbf{X}^{(1)}, \dots, \mathbf{X}^{(n)})) \\ &= H(\mathbf{X}_t|\mathbf{X}_p) \leq H(\mathbf{X}_t - \mathbf{X}_p). \end{aligned} \quad (3)$$

In conventional video coding, frame prediction \mathbf{X}_p is formed by using different predictors in different parts of the frame,

and then coding the prediction residual $\mathbf{X}_t - \mathbf{X}_p$. However, (3) says that a more efficient approach is coding \mathbf{X}_t conditionally relative to the candidate predictors. In the next section we describe a codec that is built on these principles, utilizing conditional coding and a variety of predictors.

2.2. Codec description

Fig. 1 depicts the structure of our proposed video compression system. It consists of three major components: 1) the motion coder, 2) the mode generator, and 3) the inter-frame coder. The exact functionality of each of these components is described below.

The motion coder: Given the current frame \mathbf{X}_t and its reconstructed reference frame $\hat{\mathbf{X}}_{t-1}$, we first feed them to a learned optical flow estimation network like PWC-Net [13], to obtain a motion flow map \mathbf{F}_t . The obtained flow is then encoded by the encoder (AE) of the HyperPrior-based coder from [1], and the obtained motion bitstream is transmitted to the decoder. At the decoder side, the transmitted flow map is reconstructed by the decoder (AD) of the HyperPrior coder to obtain $\hat{\mathbf{F}}_t$. Then, $\hat{\mathbf{X}}_{t-1}$ is warped by $\hat{\mathbf{F}}_t$ using bilinear sampling [16] to obtain a motion-compensated frame $\bar{\mathbf{X}}_t$.

The above-described motion coder is only used for the first P frame in each group of pictures (GOP). For the subsequent P frames, we use the CANF-based motion coder shown in Fig. 2. Here, the extrapolation network is used to extrapolate a flow map \mathbf{F}_e from the three previously-decoded frames $\hat{\mathbf{X}}_{t-3}, \hat{\mathbf{X}}_{t-2}, \hat{\mathbf{X}}_{t-1}$ and two decoded-flow maps $\hat{\mathbf{F}}_{t-2}, \hat{\mathbf{F}}_{t-1}$. \mathbf{F}_e is then used as a conditioner for coding \mathbf{F}_t . The architecture of the motion extrapolation network is the same as the one used in CANF-VC [16].

The mode generator: The goal of the mode generator is to produce additional coding modes, which can then be used by the CANF-based conditional inter-frame coder to improve RD performance. For this purpose, the previous reconstructed frame $\hat{\mathbf{X}}_{t-1}$, the motion-compensated frame $\bar{\mathbf{X}}_t$, and the de-

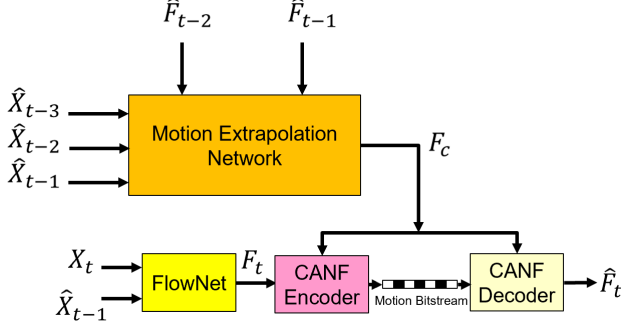


Fig. 2. The overall structure of the motion extrapolation network for producing a conditional flow, F_c , for encoding F_t .

coded flow map \hat{F}_t are concatenated and fed to the mode generator (implemented as a convolutional network, details in Section 2.3) to produce two weight maps α_t and β_t . Since these maps are produced from previously (de)coded data, they can be regenerated at the decoder without any additional bits. These two maps are then fed to a sigmoid layer to bound their values between 0 and 1. After that, a frame predictor \tilde{X}_t is generated as:

$$\tilde{X}_t = \beta_t \odot \bar{X}_t + (1 - \beta_t) \odot \hat{X}_{t-1}, \quad (4)$$

where \odot denotes Hadamard (element-wise) product and $\mathbf{1}$ is the all-ones matrix. Moreover, α_t is multiplied by both \tilde{X}_t and X_t , and the resultant two frames, $\alpha_t \odot \tilde{X}_t$ and $\alpha_t \odot X_t$, are fed to the CANF-based conditional inter-frame coder for coding $\alpha_t \odot X_t$ conditioned on $\alpha_t \odot \tilde{X}_t$. Note that α_t , β_t , \hat{X}_{t-1} and \tilde{X}_t are available at the decoder.

The inter-frame coder: The inter-frame coder codes $\alpha_t \odot X_t$ conditioned on $\alpha_t \odot \tilde{X}_t$ using the inter-frame coder of CANF-VC to obtain \tilde{X}_t at the decoder. The final reconstruction of the current frame, i.e. \hat{X}_t , is then obtained by:

$$\hat{X}_t = \tilde{X}_t + (1 - \alpha_t) \odot \tilde{X}_t. \quad (5)$$

In the limiting case when $\beta_t \rightarrow 0$, the predictor \tilde{X}_t becomes equal to \hat{X}_{t-1} , but when $\beta_t \rightarrow 1$, \tilde{X}_t becomes equal to the motion-compensated frame \bar{X}_t . For $0 < \beta_t < 1$, the predictor \tilde{X}_t is a pixel-wise mixture of \hat{X}_{t-1} and \bar{X}_t . Hence, β_t provides the system with more flexibility for choosing the predictor for each pixel within the current frame being coded. Also, for pixels where $\alpha_t \rightarrow 0$, \hat{X}_t becomes equal to \tilde{X}_t , so the inter-frame coder does not need to code anything. This resembles the SKIP mode in conventional coders, and depending on the value of β_t , the system can directly copy from \hat{X}_{t-1} , \bar{X}_t , or a mixture of these two, to obtain \hat{X}_t . When $\alpha_t \rightarrow 1$, only the inter-frame coder is used to obtain \hat{X}_t . In the limiting case when $\alpha_t \rightarrow 1$ and $\beta_t \rightarrow 1$, the proposed method would reduce to CANF-VC [16]. Hence, the proposed system has more flexibility and a larger number of conditional coding modes than CANF-VC.

Note that a somewhat similar approach was proposed in [14]. However, [14] used only one weight map, which is similar to our α map, and this map was coded and transmitted to the decoder. In our proposed system, two maps, α and β , are used to create a larger number of modes. Moreover, these two maps can be constructed using previously (de)coded information, so they can be regenerated at the decoder without any additional bits to signal the coding modes.

2.3. Implementation details

To implement the proposed system, conditional CANF-based coders from [16] are used to implement the motion coder and the inter-frame coder. The proposed mode generator is implemented as a simple convolutional network with structure $[C_1, R_1, C_2]$, where C_1 and C_2 are convolutional layers with 32 kernels of size 3×3 (stride=1, padding=1), and R_1 is a LeakyReLU layer whose negative slope is 0.1. Similar to CANF-VC, we use ANFIC [8] for encoding the I-frames.

3. EXPERIMENTS

3.1. Training

We trained the proposed LCCM-VC on the VIMEO-90K Setuplet dataset [19], which consists of 91,701 7-frame sequences with fixed resolution 448×256 , extracted from 39K selected video clips. We randomly cropped these clips into 256×256 patches, and used them for training LCCM-VC using a GOP of $N = 5$ frames. We employed the Adam [20] optimizer with the batch size of 4. We adopted a two-stage training scheme. In the first stage, we froze the CANF-based conditional coders with their pre-trained weights, and optimized the remainder of the model for 5 epochs with the initial learning rate of 10^{-4} . In the second stage, we trained the entire system end-to-end for 5 more epochs with the initial learning rate of 10^{-5} . Four separate models were trained for four different bitrates using the following loss function:

$$\mathcal{L} = \sum_{i=1}^N \frac{\eta_i}{\sum_j \eta_j} \cdot \mathcal{L}_i, \quad (6)$$

where $\eta_i = i$, and \mathcal{L}_i is the RD loss of the i -th training frame defined in [16] with $\lambda_1 \in \{256, 512, 1024, 2048\}$ and $\lambda_2 = 0.01 \cdot \lambda_1$. Note that [16] used $\mathcal{L} = \sum_i \mathcal{L}_i$ as the training loss, without weighting. In our experiments, we first trained the model with $\lambda_1 = 2048$ (highest rate), and all lower-rate models were then initialized from this model.

3.2. Evaluation methodology

We evaluate the performance of LCCM-VC on three datasets commonly-used in learning-based video coding: UVG [21] (7 sequences), MCL-JCV [22] (30 sequences), and HEVC Class B [23] (5 sequences). Following the common test protocol

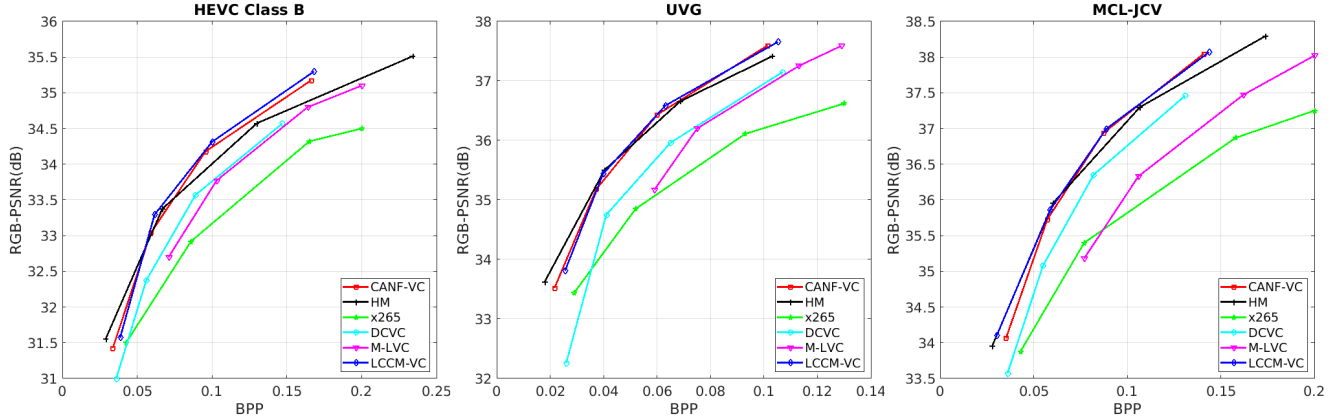


Fig. 3. Comparing various methods on three datasets: HEVC Class B, UVG, and MCL-JCV.

used in the recent literature [16], we encoded only the first 96 frames of the test videos, with the GOP size of 32.

We used the following video codecs as benchmarks: x265 (‘very slow’ mode) [24], HEVC Test Model (HM 16.22) with LDP profile [17], M-LVC [25], DCVC [26], and CANF-VC [16]. Note that CANF-VC can be considered as the current state-of-the-art learned video codec. As the quality of the I-frames has a significant role on the RD performance of video codecs, in order to have a fair comparison, we used ANFIC [8] as the I-frame coder for all learned codecs in the experiment. Note that ANFIC achieves the state-of-the-art performance for static image coding [8]. For HM and x265, we used the data points reported in [16], while for other codecs we used their original public code.

Similar to the existing practice in the learned video coding literature [16, 25, 26], to evaluate the RD performance of various methods, the bitrates were measured in bits per pixel (BPP) and the reconstruction quality was measured by RGB-PSNR. Then the RD performance is summarized into BD-Rate [27]. However, unlike related works that use x265 as the anchor, we used HM 16.22 as the anchor for computing BD-Rates. This is because HM 16.22 is a much stronger codec than x265, as will be seen in the results.

3.3. Results

In Fig. 3, we plot RGB-PSNR vs. BPP curves of various codecs on the three datasets. It is notable that both LCCM-VC and CANF-VC achieve better performance than HM 16.22 at higher bitrates/qualities, whereas HM 16.22 has slight advantage at lower bitrates. All three codecs seem to offer comparable performance at medium bitrates.

Table 1 shows BD-rate (%) relative to the HM 16.22 anchor, with negative values showing an average bit reduction (i.e., coding gain) relative to the anchor. The best result in each row of the table is shown in bold. First, note that x265, even in its ‘very slow’ mode used here, is 75-82% less efficient than HM 16.22. This is the reason why we did not use it as the anchor, but opted for HM 16.22 instead.

Table 1. BD-Rate (%) relative to HM 16.22.

Dataset	x265	DCVC	M-LVC	CANF-VC	LCCM-VC
HEVC-B	+80.80	+27.11	+28.73	+1.23	-2.78
UVG	+82.21	+52.56	+73.88	+4.04	+3.37
MCL-JCV	+75.62	+23.83	+61.16	+2.51	-1.09

The proposed LCCM-VC shows the best performance among the learning-based video codecs on all three datasets. In fact, on HEVC Class B and MCL-JCV datasets, it is even better than HM 16.22. The BD-Rate gains of LCCM-VC over CANF-VC, the second-best learned codec in this comparison, are 4.01%, 0.67%, and 3.60% on HEVC Class B, UVG, and MCL-JCV, respectively. Averaging these according to the number of videos in each dataset gives the average BD-Rate gain of 3.16%. Although LCCM-VC uses the same conditional coding engines as CANF-VC, it benefits from more flexible coding modes, as explained in Section 2, and thereby achieves better RD performance.

4. CONCLUSIONS

In this paper, we proposed learned conditional coding modes for video coding (LCCM-VC), an end-to-end learned video codec that, to our knowledge, achieves state-of-the-art results among learning-based codecs. We also gave a theoretical justification for why conditional coding relative to multiple coding modes should be better than residual coding. LCCM-VC outperforms other learning-based video codecs on three commonly used test datasets, and even outperforms HM 16.22 on two of these datasets.

5. ACKNOWLEDGMENT

We would like to thank the authors of CANF-VC [16] for fruitful discussions and for sharing their code, which has formed the basis of the proposed method.

6. REFERENCES

- [1] J. Ballé, D. Minnen, S. Singh, S. J. Hwang, and N. Johnston, “Variational image compression with a scale hyperprior,” in *Intl. Conf. on Learning Representations (ICLR)*, 2018, pp. 1–23.
- [2] D. Minnen, J. Ballé, and G. D. Toderici, “Joint autoregressive and hierarchical priors for learned image compression,” in *Advances in Neural Information Processing Systems*, 2018, vol. 31.
- [3] Z. Cheng, H. Sun, M. Takeuchi, and J. Katto, “Learned image compression with discretized gaussian mixture likelihoods and attention modules,” in *Proceedings of the IEEE Conference on Computer Vision and Pattern Recognition (CVPR)*, 2020.
- [4] G. J. Sullivan, J. R. Ohm, W. J. Han, and T. Wiegand, “Overview of the high efficiency video coding (HEVC) standard,” *IEEE Trans. Circuits and Systems for Video Technology*, vol. 22, no. 12, 2012.
- [5] B. Bross, Y. K. Wang, Y. Ye, S. Liu, J. Chen, G. J. Sullivan, and J. R. Ohm, “Overview of the versatile video coding (VVC) standard and its applications,” *IEEE Trans. Circuits and Systems for Video Technology*, vol. 31, no. 10, 2021.
- [6] J. Lee, S. Cho, and S. K. Beack, “Context-adaptive entropy model for end-to-end optimized image compression,” in *Intl. Conf. on Learning Representations (ICLR)*, 2019.
- [7] L. Helming, A. Djelouah, M. Gross, and C. Schroers, “Lossy image compression with normalizing flows,” in *Intl. Conf. on Learning Representations (ICLR)*, 2021.
- [8] Y. H. Ho, C. C. Chan, W. H. Peng, H. M. Hang, and M. Domanski, “ANFIC: Image compression using augmented normalizing flows,” *IEEE Open Journal of Circuits and Systems*, vol. 2, pp. 613–626, 2021.
- [9] G. Lu, W. Ouyang, D. Xu, X. Zhang, C. Cai, and Z. Gao, “DVC: An end-to-end deep video compression framework,” in *Proceedings of the IEEE/CVF Conference on Computer Vision and Pattern Recognition*, 2019, p. 11006–11015.
- [10] E. Agustsson, D. Minnen, N. Johnston, Ballé J., Hwang S. J., and G. Toderici, “Scale-space flow for end-to-end optimized video compression,” in *Proceedings of the IEEE/CVF Conference on Computer Vision and Pattern Recognition*. IEEE, 2020, pp. 8503–8512.
- [11] H. Liu, M. Lu, Z. Ma, F. Wang, Z. Xie, X. Cao, and Y. Wang, “Neural video coding using multiscale motion compensation and spatiotemporal context model,” *IEEE Trans. Circuits and Systems for Video Technology*, 2020.
- [12] Z. Hu, G. Lu, and D. Xu, “FVC: A new framework towards deep video compression in feature space,” in *Proceedings of the IEEE/CVF Conference on Computer Vision and Pattern Recognition*, 2021, p. 1502–1511.
- [13] D. Sun, X. Yang, M. Y. Liu, and J. Kautz, “PWC-Net: CNNs for optical flow using pyramid, warping, and cost volume,” in *Proceedings of the IEEE conference on computer vision and pattern recognition*, 2018, p. 8934–8943.
- [14] T. Ladune, P. Philippe, W. Hamidouche, L. Zhang, and O. Déforges, “Optical flow and mode selection for learning-based video coding,” in *IEEE 22nd International Workshop on Multimedia Signal Processing*, 2020.
- [15] T. Ladune, P. Philippe, W. Hamidouche, L. Zhang, and O. Déforges, “Conditional coding for flexible learned video compression,” in *Neural Compression From Information Theory to Applications—Workshop@ ICLR 2021*, 2021.
- [16] Y. H. Ho, C. P. Chang, P. Y. Chen, A. Gnutti, and W. H. Peng, “CANF-VC: Conditional augmented normalizing flows for video compression,” *European Conference on Computer Vision*, 2022.
- [17] HM, “Reference software for HEVC,” https://vcgit.hhi.fraunhofer.de/Zhu/HM/blob/HM-16.22/cfg/encoder_lowdelay_P_main.cfg, 2022-03-10.
- [18] T. M. Cover and J. A. Thomas, *Elements of Information Theory*, Wiley, 2nd edition, 2006.
- [19] T. Xue, B. Chen, J. Wu, D. Wei, and W. T. Freeman, “Video enhancement with task-oriented flow,” *International Journal of Computer Vision*, vol. 127, no. 8, pp. 1106–1125, 2019.
- [20] D. P. Kingma and J. Ba, “Adam: A method for stochastic optimization,” in *International Conference for Learning Representations*, 2015.
- [21] A. Mercat, M. Viitanen, and J. Vanne, “UVG dataset: 50/120fps 4k sequences for video codec analysis and development,” in *Proceedings of the 11th ACM Multimedia Systems Conference*, 2020, pp. 297–302.
- [22] H. Wang, W. Gan, S. Hu, J. Y. Lin, L. Jin, L. Song, P. Wang, I. Katsavounidis, A. Aaron, and C. C. J. Kuo, “MCL-JCV: a JND-based H.264/AVC video quality assessment dataset,” in *2016 IEEE International Conference on Image Processing (ICIP)*, 2016, pp. 1509–1513.
- [23] Frank B., “Common test conditions and software reference configurations,” in *JCTVC-L1100 12(7)*, 2013.
- [24] x265, “An open-source HEVC encoder,” <https://x265.readthedocs.io/en/master/>, 2022-03-10.
- [25] J. Lin, D. Liu, H. Li, and F. Wu, “M-LVC: multiple frames prediction for learned video compression,” in *Proceedings of the IEEE/CVF Conference on Computer Vision and Pattern Recognition*, 2020, p. 3546–3554.
- [26] J. Li, B. Li, and Y. Lu, “Deep contextual video compression,” in *Advances in Neural Information Processing Systems*, 2021.
- [27] G. Bjøntegaard, “Calculation of average PSNR differences between RD-curves,” Apr. 2001, VCEG-M33.